

Monitoring the effects of silica fume, copper slag and nano-silica on the mechanical properties of polypropylene fiber-reinforced cementitious composites

Moosa Mazloom^{*1}, Hasan Salehi^{2a} and Mohammad Akbari-Jamkarani^{1b}

¹Department of Structural and Earthquake Engineering, Faculty of Civil Engineering, Shahid Rajaee Teacher Training University, I. R. Iran

²Department of Mechanical Engineering, Khatam Ol Anbia University, Tehran, Iran

(Received May 20, 2024, Revised June 12, 2024, Accepted June 15, 2024)

Abstract. In this study, to reduce the amount of cement consumed in the production of cementitious composites, the effects of partial replacement of cement weight with nano-silica, silica fume, and copper slag on the mechanical properties of polypropylene fiber-reinforced cementitious composites are investigated. For this purpose, the effect of replacing cement weight by each of the aforementioned materials individually and in combination is studied. A total of 34 mix designs were prepared, and their compressive, tensile, and flexural strengths were obtained for each mix. Among the mix designs with one cement replacement material, the highest strength is related to the sample containing 2.5% nano-silica. In this mix design, the compressive, tensile, and flexural strengths improve by about 33%, 13%, and 15%, respectively, compared to the control sample. In the ones with two cement replacement materials, the highest strengths are related to the mix made with 10% silica fume along with 2% nano-silica. In this mix design, compressive, tensile, and flexural strengths increase by about 42%, 18%, and 20% compared to the control sample, respectively. Furthermore, in the mixtures containing three cement substitutes, the final optimal mix design for all three strengths has 15% silica fume, 10% copper slag, and 2% nano-silica. This mix design improves the compressive, tensile, and flexural strengths by about 57%, 23%, and 26%, respectively, compared to the control sample. Finally, two relationships have been presented that can be used to predict the values of tensile and flexural strengths of cementitious composites with very good accuracy only by determining the compressive strength of the composites.

Keywords: cementitious composite; copper slag; mechanical properties; nano-silica; silica fume; polypropylene fiber

1. Introduction

Concrete is one of the most widely used building materials and the production of which is increasing day by day. Despite the many advantages of this material, one of the weaknesses of it is its low tensile strength (Salehi and Mazloom 2018). Concrete is prone to cracking due to its low

*Corresponding author, Professor, E-mail: Mazloom@sru.ac.ir

^aAssistant Professor, E-mail: h.salehi@sru.ac.ir

^bMSc Student, E-mail: mohammad.akbari@sru.ac.ir

tensile and bending strength (Salehi and Mazloom 2019). After cracking, the concrete stress-bearing capacity decreases significantly, and as a result, its strength, hardness, and durability decrease (Mazloom and Salehi 2018).

The increasing demand for the structural use of concrete requires that researchers study leads to the construction of concretes that not only have more ductile behavior but can also absorb the energy caused by extreme loads. Cementitious composites have good plasticity, but due to having a large amount of cement, the happening extensive micro cracks with different dimensions are likely. According to prior studies, adding fibers to a volume ratio of 2% can increase the tensile strain capacity by 3 to 5% (Le Hoang and Fehling 2017). Under cyclic loading, fiber-reinforced cement composite members absorb more energy than standard reinforced concrete members (Shajil, Srinivasan *et al.* 2013, Gideon and Milan 2021). Therefore, to increase the durability and service life of concrete structures under severe cyclic loading, it is necessary to use fibers that can undergo large deformations while maintaining their ductile behavior as reinforcement.

To improve the brittle behavior of concrete and prevent the extension of cracks, fiber reinforced concrete (FRC) was made by adding fibers to the paste. Therefore, in many studies, fibers have been used as micro-reinforcement to prevent cracks and increase the durability of concrete (van Zijl *et al.* 2012, Mazloom *et al.* 2020). The fibers used to prevent the expansion and opening of the crack (Aydin 2007). These fibers have different types, one of which is polymer fibers. There are different types of polymer fibers, and their resistance is considerable (Gao *et al.* 2010). Huang (2001) stated that using polymer fibers in alkaline and chemical environments increases concrete durability and mechanical properties. One of the types of these polymer fibers is polypropylene fibers. Adding polypropylene fibers to the mixture increases the compressive, tensile, and bending strengths of the cement composites (Mazaheripour *et al.* 2011, Mardani-Aghabaglou *et al.* 2013). Due to the dimensions and geometry of polypropylene fibers, they reduced the efficiency of concrete (Kakooei *et al.* 2012).

The mixes of fiber cement composites usually have a very high cement content. To preserve the environment, the requirement to reduce cement consumption in the mix designs seems logical. To decrease cement consumption, substituting cement with pozzolans can be useful (Yu *et al.* 2018, Ghalehnovi *et al.* 2022). One of the types of pozzolans is the silica fume. Silica fume increases resistance to melting and freezing cycles. Furthermore, adding silica fume has a desirable effect on the mix's compressive strength even at high temperatures (Massana *et al.* 2018, Mazloom and Mirzamohammadi 2021). Studies show that using concrete mix containing 10% silica fume can improve the durability of reinforcement against corrosion and the useful life of marine structures (Tangtakabi *et al.* 2022). Mazloun *et al.* (2018) stated that silica fume reduces trapped air in ordinary and self-compacting concrete. They also investigated the effect of silica fume on self-compacting lightweight concrete and reported that this material increases the durability and mechanical properties of this concrete. Existing silica fume causes many pozzolanic reactions and affects the strength parameters (Mazloom *et al.* 2017, Saha *et al.* 2017). Furthermore, adding silica fume to concrete accelerates hydration and increases compressive strength (Mazloom and Salehi 2018, Salehi and Mazloom 2019).

Another important pozzolan is nano-silica. Among these two materials, silica fume is more abundant and is considered one of the available and popular micro-scale pozzolans. But in recent years, due to the development of the industry, nano-scale particles have been used more in concrete research (Amiri *et al.* 2022). These particles have desirable effects on cement-based composites due to their small particle and excellent pozzolanic properties (Afzali-Naniz and Mazloom 2019, Abna and Mazloom 2022). Elahi *et al.* (2010) investigated the effect of silica fume

and nano-silica on concrete. They found that the pozzolanic activity of nano-silica is more than that of the silica fume. Therefore, nano-silica improves the mechanical properties of concrete more than silica fume. Massana *et al.* (2018) showed that due to the pozzolanic properties of nano-silica, adding it increases compressive strength and decreases the permeability of hardened concrete. Nano-silica can increase the concrete density by reducing the voids in the cement matrix. Furthermore, using nano-silica in the production of concrete leads to a decrease in water absorption and permeability and increases the resistance of concrete against acid attack (Kashyap *et al.* 2022). In general, using nano-silica as a cement substitute in concrete can reduce CO₂ emissions from cement production and reduce environmental risks.

Another pozzolan used in concrete is copper furnace slag. Copper slag produced by mining industries and copper recycling factories is about 50 million tons annually, which is one of the biggest environmental challenges (Edwin *et al.* 2022). Copper slag is classified as hazardous waste due to existing harmful elements such as arsenic, cadmium, chromium, lead, and zinc. Therefore, the use of copper slag in the production of concrete is the most effective method that can be used to use this dangerous waste and simultaneously solve the problem of environmental destruction and construction cost. Adding copper slag to cement mixtures increases the flowability and compressive strength of the mix (Murari *et al.* 2015, Mazloom *et al.* 2022). Wang *et al.* (2016) showed that the mechanical properties increased by replacing copper slag instead of sand. Lim *et al.* (2017) investigated the mechanical and hydraulic properties of the concrete by substituting copper slag instead of cement. They acknowledged that the best mix design contained 60% copper slag, and this mix improved the strength parameters of concrete by about 20%. Dos Anjos *et al.* (2017) also investigated the mechanical properties of high-strength concrete by replacing copper slag with the coarse aggregate. They showed that using copper slag increases the compressive and tensile strength of the concrete by a maximum of about 10%. Copper slag affects the mechanical characteristics of concrete according to the ratio of water to cement and the amount of slag replacements (Feng *et al.* 2019). In this regard, some studies claimed that replacing more than 30% of copper slag in the concrete mixture causes its quality to decrease (Tiwary and Bhatia 2022).

Therefore, due to the different properties of ordinary concrete and cement composites, in this research, by examining the design of multiple variables and performing non-linear regression, relationships have been presented that only by determining the compressive strength of the mix design the values of tensile and flexural strengths of cement composites can be predicted. Also, according to the mentioned technical literature and based on the analysis of the studies, in this research, to reduce the amount of cement consumed in the production of cementitious composites, in addition to silica fume, nano silica, and copper slag have been used. In this regard, the effect of replacing nano-silica, silica fume, and copper slag individually and in combination on the mechanical properties of cementitious composites reinforced with polypropylene fibers has been investigated. In this way, by conducting an extensive study and examining many mix designs, the best substitute material for cement has been introduced to increase the mechanical properties of cementitious composites. Moreover, their optimal replacement level has been expressed in the case of using individually or blended, so that they can be used in the next studies and structural projects as the optimal cases to reduce cement consumption.

2- Materials

The mix designs used in this study contain cement, water, silica fume, nano-silica, copper slag,

silica sand, polypropylene fibers, and superplasticizer. To increase the flow ability of the mixtures was used a polycarboxylate-based superplasticizer. The specifications of the superplasticizer based on the ASTM-C494 standard (2001) are shown in Table 1. The technical and physical characteristics of nano-silica and fibers are shown in Tables 1 and 2. Silica fume was obtained from the Ferrosilicon Shahriar factory. Portland cement type 425-1, silica fume, and copper slag had a specific gravity of 3.07, 2.5, and 1.75 grams per cubic centimeter, respectively, and their chemical characteristics are presented in Table 3.

3. Mix design and testing method

The mix design of cementitious composites containing fibers is shown in the form of weight percentage in Table 4, which includes 34 mix designs. Mix 1 is the control sample, mixes 2 to 5 include 5, 7, 10, and 15 percent of silica fume, and mixes 6 to 9 include 5, 10, 20, and 30 percent of copper slag. Mixes 10 to 14 contain 1, 1.5, 2 and 2.5 percent of nano-silica, and mixes 15 to 18 have 10 and 15 percent silica fume along with 10 and 20 percent copper slag. Mixes 19 to 24 have 10 and 15 percent silica fume along with 1.5, 2, and 2.5 percent nano-silica. Mixes 25 to 30 have 10 and 20% copper slag along with 1.5, 2, and 2.5% nano-silica, and finally mixes 31 to 34 have 15% silica fume, 10 and 20% copper slag along with 2 and 2.5% nano-silica.

To prepare the samples, at first silica sand was mixed with all the fibers inside the mixer for 5 minutes, and then the materials were added from fine to coarse and mixed for 1 minute. Finally, water and Super-plasticizer were added and mixed for 3 minutes. After one day, the molds were opened, and samples were kept in lime-saturated water solution at a temperature of about 20 ± 2 until the time of the experiment. They were cured for 27 days and ready for testing. Three cement replacement materials, including silica fume, nano silica and copper slag were used in this research.

Table 1 Technical specifications of nano-silica and superplasticizer

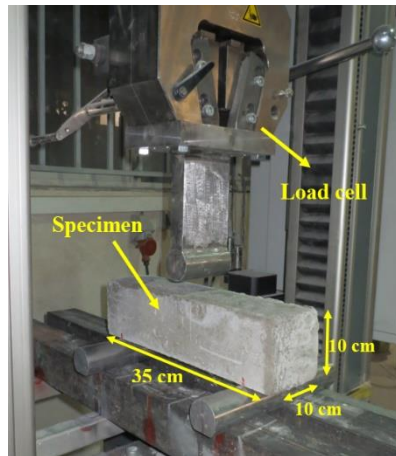
| Specifications | Nano-silica | Superplasticizer |
|-------------------------------|-------------|------------------|
| appearance | milky | light brown |
| specific weight (gr/cm^3) | 1.4 | 1.11 |
| pH | 9.3 | 6.8 |
| particle size (nm) | 10-30 | - |
| chlorine ion | - | less than 0.1% |

Table 2 Properties of polypropylene fibers

| Characteristics | Results |
|-------------------------------|---------|
| Specific weight (kg/m^3) | 910 |
| Tensile strength (MPa) | 400 |
| Melting Point ($^{\circ}C$) | 165 |
| Length (mm) | 12 |
| Diameter (nm) | 23 |
| Elastic modulus (GPa) | 2.7 |

Table 3 Chemical characteristics of Portland cement, silica fume, nano-silica, copper slag and silica sand

| Compounds | Portland cement (%) | Silica fume (%) | nano-silica (%) | Copper slag (%) | Silica sand (%) |
|--------------------------------|---------------------|-----------------|-----------------|-----------------|-----------------|
| SiO ₂ | 21.30 | 95.04 | 96.4 | 34 | 98.10 |
| CaO | 63.48 | 0.49 | 0.49 | 6.50 | 0.06 |
| Al ₂ O ₃ | 5.13 | 1.32 | 1.32 | 3.65 | 1.10 |
| Fe ₂ O ₃ | 3.47 | 0.67 | 0.87 | - | 0.10 |
| Na ₂ O | 0.23 | 0.21 | 0.31 | - | 0.40 |
| MgO | 3.51 | 0.97 | 0.97 | 1.51 | - |
| P ₂ O ₅ | - | 0.16 | 0.16 | - | - |
| SO ₃ | 1.87 | 0.10 | 0.10 | - | - |
| K ₂ O | 0.56 | 1.01 | 1.01 | - | 0.40 |
| SiC | - | 0.50 | 0.50 | - | - |
| C | - | 0.30 | 0.30 | - | - |
| CL | 0.04 | - | 0.04 | 0.03 | - |
| H ₂ O | - | 0.08 | 0.08 | - | - |
| FeO | - | - | - | 54 | - |
| CuO | - | - | - | 0.70 | - |
| Sulfate | - | - | - | 0.02 | - |



(a)



(b)

Fig. 1 The overview of (a) Bending strength test under the servo electro-controlled universal machine and (b) Compressive strength test under the hydraulic pressure machine

To name the mix designs, silica fume is shown with S, nano-silica with N, and copper slag with C. The samples were subjected to compressive, tensile and bending strength tests.

As shown in Fig. 1, an ELE 200 t compressive test machine was used to test the compressive and tensile strengths of the cementitious composite samples. The compressive strength was tested according to the BSI-12390 standard (2001) on 10 cm standard cubes. The loading rate of this test

Table 4 Mix design of fiber-reinforced cementitious composites samples (kg/m^3)

| Number | Sample label | Cement | Silica fume | Copper slag | Nano-silica | Silica sand | Fiber | Water | Super-plasticizer |
|--------|--------------|--------|-------------|-------------|-------------|-------------|-------|-------|-------------------|
| 1 | plain | 1120 | 0 | 0 | 0 | 589.5 | 21.45 | 313.6 | 29.5 |
| 2 | S5 | 1064 | 56 | 0 | 0 | 589.5 | 21.45 | 313.6 | 29.5 |
| 3 | S7 | 1041.6 | 78.4 | 0 | 0 | 589.5 | 21.45 | 313.6 | 29.5 |
| 4 | S10 | 1008 | 112 | 0 | 0 | 589.5 | 21.45 | 313.6 | 29.5 |
| 5 | S15 | 952 | 168 | 0 | 0 | 589.5 | 21.45 | 313.6 | 29.5 |
| 6 | C5 | 1064 | 0 | 56 | 0 | 589.5 | 21.45 | 313.6 | 29.5 |
| 7 | C10 | 1008 | 0 | 112 | 0 | 589.5 | 21.45 | 313.6 | 29.5 |
| 8 | C20 | 896 | 0 | 224 | 0 | 589.5 | 21.45 | 313.6 | 29.5 |
| 9 | C30 | 784 | 0 | 336 | 0 | 589.5 | 21.45 | 313.6 | 29.5 |
| 10 | N1 | 1108.8 | 0 | 0 | 11.2 | 589.5 | 21.45 | 313.6 | 29.5 |
| 11 | N1.5 | 1103.2 | 0 | 0 | 16.8 | 589.5 | 21.45 | 313.6 | 29.5 |
| 12 | N2 | 1097.6 | 0 | 0 | 22.4 | 589.5 | 21.45 | 313.6 | 29.5 |
| 13 | N2.5 | 1092 | 0 | 0 | 28 | 589.5 | 21.45 | 313.6 | 29.5 |
| 14 | N3 | 1086.4 | 0 | 0 | 33.6 | 589.5 | 21.45 | 313.6 | 29.5 |
| 15 | S10C10 | 896 | 112 | 112 | 0 | 589.5 | 21.45 | 313.6 | 29.5 |
| 16 | S15C10 | 840 | 168 | 112 | 0 | 589.5 | 21.45 | 313.6 | 29.5 |
| 17 | S10C20 | 784 | 112 | 224 | 0 | 589.5 | 21.45 | 313.6 | 29.5 |
| 18 | S15C20 | 728 | 168 | 224 | 0 | 589.5 | 21.45 | 313.6 | 29.5 |
| 19 | S10N1.5 | 991.2 | 112 | 0 | 16.8 | 589.5 | 21.45 | 313.6 | 29.5 |
| 20 | S10N2 | 958.6 | 112 | 0 | 22.4 | 589.5 | 21.45 | 313.6 | 29.5 |
| 21 | S10N2.5 | 980 | 112 | 0 | 28 | 589.5 | 21.45 | 313.6 | 29.5 |
| 22 | S15N1.5 | 935.2 | 168 | 0 | 16.8 | 589.5 | 21.45 | 313.6 | 29.5 |
| 23 | S15N2 | 929.6 | 168 | 0 | 22.4 | 589.5 | 21.45 | 313.6 | 29.5 |
| 24 | S15N2.5 | 924 | 168 | 0 | 28 | 589.5 | 21.45 | 313.6 | 29.5 |
| 25 | C10N1.5 | 991.2 | 0 | 112 | 16.8 | 589.5 | 21.45 | 313.6 | 29.5 |
| 26 | C10N2 | 985.6 | 0 | 112 | 22.4 | 589.5 | 21.45 | 313.6 | 29.5 |
| 27 | C10N2.5 | 980 | 0 | 112 | 28 | 589.5 | 21.45 | 313.6 | 29.5 |
| 28 | C20N1.5 | 879.2 | 0 | 224 | 16.8 | 589.5 | 21.45 | 313.6 | 29.5 |
| 29 | C20N2 | 873.6 | 0 | 224 | 22.4 | 589.5 | 21.45 | 313.6 | 29.5 |
| 30 | C20N2.5 | 868 | 0 | 224 | 28 | 589.5 | 21.45 | 313.6 | 29.5 |
| 31 | S15C10N2 | 817.6 | 168 | 112 | 22.4 | 589.5 | 21.45 | 313.6 | 29.5 |
| 32 | S15C10N2.5 | 812 | 168 | 112 | 28 | 589.5 | 21.45 | 313.6 | 29.5 |
| 33 | S15C20N2 | 705.6 | 168 | 224 | 22.4 | 589.5 | 21.45 | 313.6 | 29.5 |
| 34 | S15C20N2.5 | 700 | 168 | 224 | 28 | 589.5 | 21.45 | 313.6 | 29.5 |

was considered 0.3 MPa/s (BSI-12390 2001). The tensile strength test was performed on cylindrical samples with a diameter and length of 15×30 cm, and the ASTM-C496 standard (2002) was used for it. In this test, a cylindrical sample was placed horizontally under a 200-ton hydraulic machine, and the loading continued continuously at a constant rate of 0.02 MPa/s until the sample broke. Thus, the maximum force (P) that can be tolerated by the sample is determined and then the tensile strength is calculated using the following relationship (ASTM-C496 2002)

$$f_t = \frac{2P}{\pi ld} \quad (1)$$

Table 5 Compressive, tensile and flexural strength tests result of the cementitious composites containing one cement substitute materials

| Number | Mix ID | Compressive strength (MPa) | Tensile strength (MPa) | Flexural strength (MPa) |
|--------|--------|----------------------------|------------------------|-------------------------|
| 1 | plain | 42.38 | 3.20 | 5.35 |
| 2 | S5 | 45.93 | 3.36 | 5.75 |
| 3 | S7 | 47.11 | 3.40 | 5.82 |
| 4 | S10 | 48.99 | 3.44 | 5.85 |
| 5 | S15 | 52.43 | 3.50 | 5.94 |
| 6 | C5 | 45.04 | 3.31 | 5.69 |
| 7 | C10 | 47.23 | 3.46 | 5.80 |
| 8 | C20 | 49.42 | 3.34 | 5.58 |
| 9 | C30 | 36.73 | 3.11 | 5.26 |
| 10 | N1 | 47.57 | 3.41 | 5.84 |
| 11 | N1.5 | 51.12 | 3.47 | 5.91 |
| 12 | N2 | 53.94 | 3.53 | 5.97 |
| 13 | N2.5 | 56.54 | 3.61 | 6.15 |
| 14 | N3 | 55.30 | 3.44 | 5.84 |

where l is the length and d is the diameter of the cylindrical sample. To determine the bending strength of different mixes, a three-point bending test was performed on samples with dimensions of $10 \times 10 \times 35$ cm. According to Fig. 1, a servo electro-controlled universal machine with a maximum capacity of 150 kN was used to perform this test. Based on the ASTM C1609 standard (2019), the loading speed was considered equal to 0.5 mm/min.

4. Results

The mechanical properties of the samples, including compressive, tensile and flexural strengths are shown in Tables 5 and 6. Figs. 2-4 show the percentage changes in compressive strength of different mixes compared to plain mixt and the normalized values of the tensile and flexural strengths based on the control sample so that their evaluation is possible visually.

4.1 Compressive strength

In Tables 5 and 6 the results of the compressive strength test and in the diagram of Fig. 2 the percentage changes in the compressive strength of different mix designs compared to the control sample are shown.

The compressive strength of each mix design is determined based on the average strengths of three cubic samples. The compressive strength of the samples was obtained in the range of 36.7 to 66.4 MPa. Based on the results, the compressive strength of all samples containing silica fume was higher than the control sample. By increasing the replacement rate of silica fume from zero to 15% of the cement weight, the compressive strength value increased gradually, and its highest value was obtained in the replacement ratio of 15%, which was about 24% more than the control sample.

Table 6 Compressive, tensile and flexural strength tests result of the cementitious composites containing the combination of different cement substitute materials

| Number | Mix ID | Compressive strength (MPa) | Tensile strength (MPa) | Flexural strength (MPa) |
|--------|------------|----------------------------|------------------------|-------------------------|
| 1 | S10C10 | 49.85 | 3.40 | 5.92 |
| 2 | S15C10 | 51.78 | 3.53 | 6.11 |
| 3 | S10C20 | 54.09 | 3.47 | 6.14 |
| 4 | S15C20 | 56.10 | 3.58 | 6.18 |
| 5 | S10N1.5 | 55.78 | 3.66 | 6.20 |
| 6 | S10N2 | 60.04 | 3.79 | 6.42 |
| 7 | S10N2.5 | 58.18 | 3.74 | 6.28 |
| 8 | S15N1.5 | 57.33 | 3.71 | 6.28 |
| 9 | S15N2 | 59.20 | 3.74 | 6.36 |
| 10 | S15N2.5 | 54.13 | 3.59 | 6.11 |
| 11 | C10N1.5 | 53.82 | 3.71 | 6.07 |
| 12 | C10N2 | 55.87 | 3.50 | 6.28 |
| 13 | C10N2.5 | 57.50 | 3.57 | 6.13 |
| 14 | C20N1.5 | 51.92 | 3.55 | 6.06 |
| 15 | C20N2 | 54.15 | 3.44 | 5.84 |
| 16 | C20N2.5 | 55.51 | 3.69 | 5.91 |
| 17 | S15C10N2 | 66.42 | 3.94 | 6.75 |
| 18 | S15C10N2.5 | 64.78 | 3.88 | 6.54 |
| 19 | S15C20N2 | 64.26 | 3.82 | 6.50 |
| 20 | S15C20N2.5 | 62.73 | 3.75 | 6.36 |

Substitution of nano-silica up to 2.5% of the cement weight caused a 33% increase in the compressive strength of the samples, and a further increase in the amount of replacement up to 3% of the cement weight decreased its desired effect by 30%. Regarding the use of copper slag, the same trend existed but with greater intensity, so that by replacing 20 and 30% of the cement weight with copper slag, the compressive strength increased by about 17% and decreased by about 13%, respectively.

Increasing the compressive strength of the mixes can be due to the fact that silica fume and copper slag act as fillers on the one hand and cause an increase in sample density, on the other hand, as activators, they accelerate pozzolanic reactions (Jalal *et al.* 2012, Mazloom *et al.* 2015, Salehi and Mazloom 2021). Based on the results, it is clear that the replacement of very low percentages of nano-silica compared to large amounts of silica fume can improve the compressive strength of the samples (Scrivener and Kirkpatrick 2008, Li *et al.* 2017). Studies conducted on mortar and self-compacting concrete show that adding a combination of nano-silica and silica fume improves the properties of the samples better than adding only one of them (Jalal *et al.* 2012, Li *et al.* 2017). Therefore, in the next step, to investigate the effect of the combination of silica fume, nano-silica and copper slag, their effect was investigated in two-by-two and three-way. Since the replacement amounts of 3% nano-silica and 30% copper slag alone also had a weaker performance than other amounts, the presence of the above percentages in the design of mixed

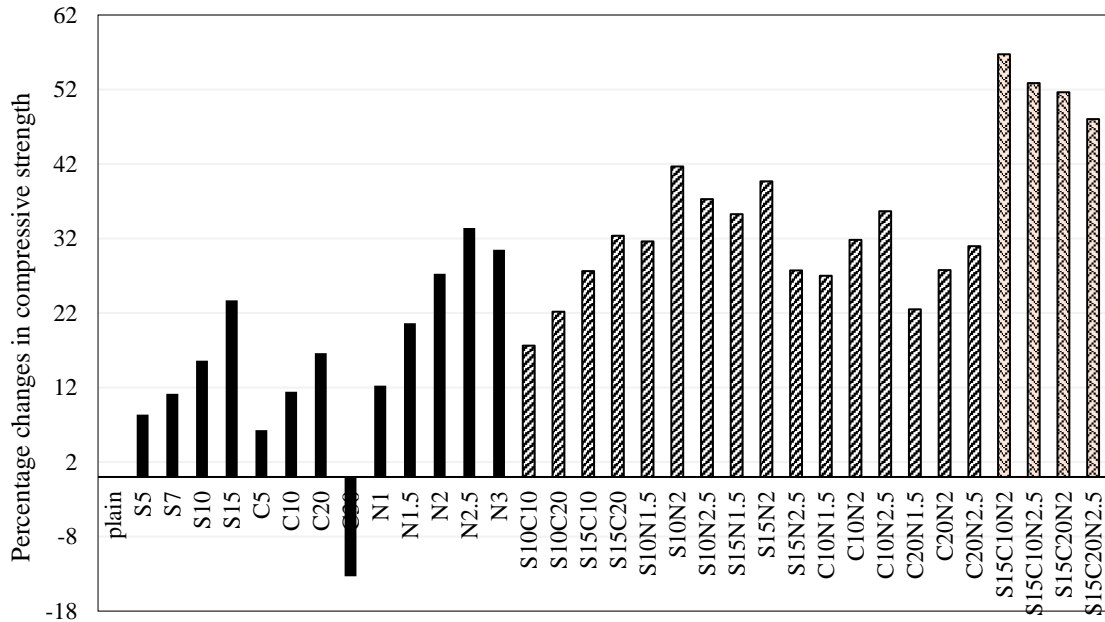


Fig. 2 Percentage changes in compressive strength of different mix designs compared to the control sample

mixtures was omitted. In the C30 mix, the percentage change of compressive strength is below of zero line, which indicates about 14% negative effect compared to the control sample.

In this study, by replacing only one of the silica fume or copper slag materials instead of cement, their optimal amount was obtained as 15 and 20%, respectively. By testing different amounts of these two materials in a combined state, it was determined that the optimal mixture is obtained by replacing 15 and 20% of the cement weight with silica fume and copper slag, respectively. In this case, the compressive strength of the S15C20 sample increases by about 32% compared to the control sample.

The simultaneous addition of nano-silica and silica fume to the mixture improves the microstructure of concrete. The reason is that silica fume is much finer than cement and fills the spaces between particles. On the other hand, nano-silica particles are even finer than silica fume and can well fill the remaining empty spaces in the mixture (Li *et al.* 2017). At the time of using one cement substitute, the optimal proportion of using nano-silica was 2.5%, which at this stage and in the combination of silica fume and nano-silica, its optimal amount changes to 2%; So by replacing 2% of nano-silica in combination with 10% and 15% of silica fume in the mix design, the compressive strength increases by about 42% and 40%, respectively. During the combination of copper slag and nano-silica, a similar behavior was observed. In this case, by replacing 2.5% of nano-silica and 10% of copper slag in the mixed design, the compressive strength of the composite sample increases by about 36%.

Therefore, based on Fig. 2 and the above results, nano-silica had the best effect in increasing strength among the mixes with one cement substitute. This is due to its purity, smaller particles, and higher pozzolanic properties. The compressive strength of the mixes design with two cement substitutes was often higher than mixes with one cement substitute. In this group, the best mix design includes the combination of silica fume and nano-silica, which improves compressive

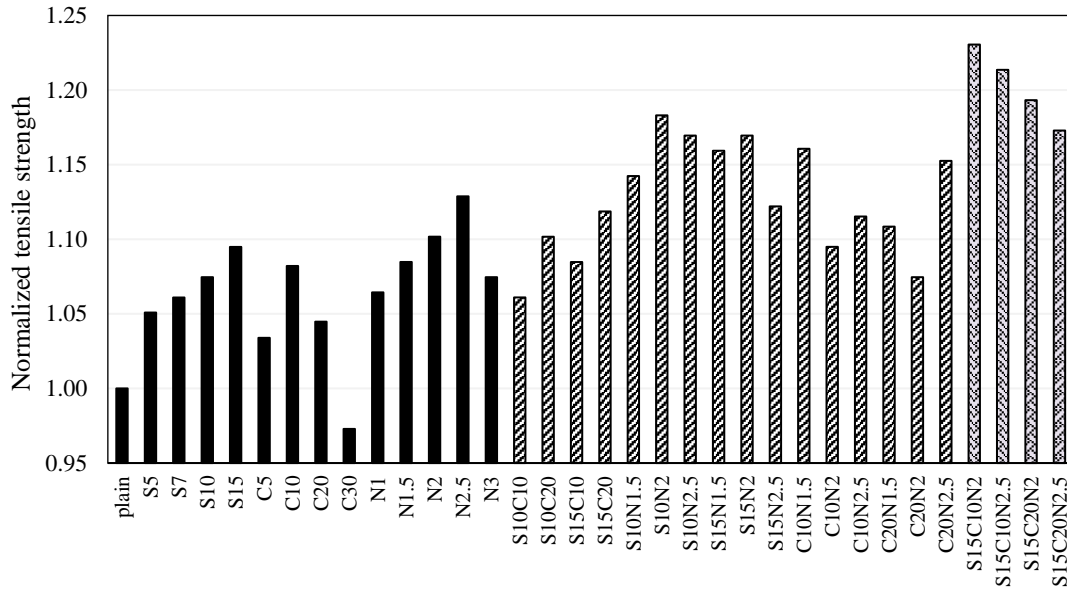


Fig. 3 Normalized tensile strength diagram according to the control sample

strength by about 42%. However, with the combination of copper slag and nano-silica, this quality improvement is slightly reduced and reaches about 36%. But this mix design has a lower cost than the previous section. Furthermore, it has better environmental effects.

Improving compressive strength in ternary mixtures replacing cement was much better than in other samples. It should be noted that increasing the content of cement replacement by copper slag from 10 to 20% (in the same proportion as silica fume and nano-silica) decreased the compressive strength of the samples. This observation can be due to the accumulation of SiO_2 particles in the concrete microstructure, which caused the formation of a weak interfacial transition zone (Kong *et al.* 2013, Nili and Ehsani 2015). The final optimal mix design included 15% silica fume, 10% copper slag, and 2% nano-silica and increased the compressive strength of the sample by about 57% compared to the control sample.

4.2 Tensile strength

The results of the tensile strength test of the samples are shown in Tables 5 and 6, and the normalized tensile strength diagram of the mix designs according to the control sample is shown in Fig. 3. The tensile strength of all mixes containing silica fume and nano-silica was higher than the control sample. In mix design with different amounts of silica and nano-silica, the mixture containing 15% silica fume with about 10% increase in tensile strength and the mix design, including 2.5% nano-silica with about 13% increase had the best performance. Meanwhile, adding copper slag up to 10% of the cement weight increased the tensile strength by about 8%, and adding this amount to 20 and 30% of the cement weight reduced its effect to the positive 5% and negative 3%, respectively. These findings are consistent with Jalal *et al.*'s study results (Jalal *et al.* 2012).

In the samples with two cement substitutes, like the compressive strength, the mix design containing 10% silica fume and 2% nano-silica had the highest tensile strength. This sample was

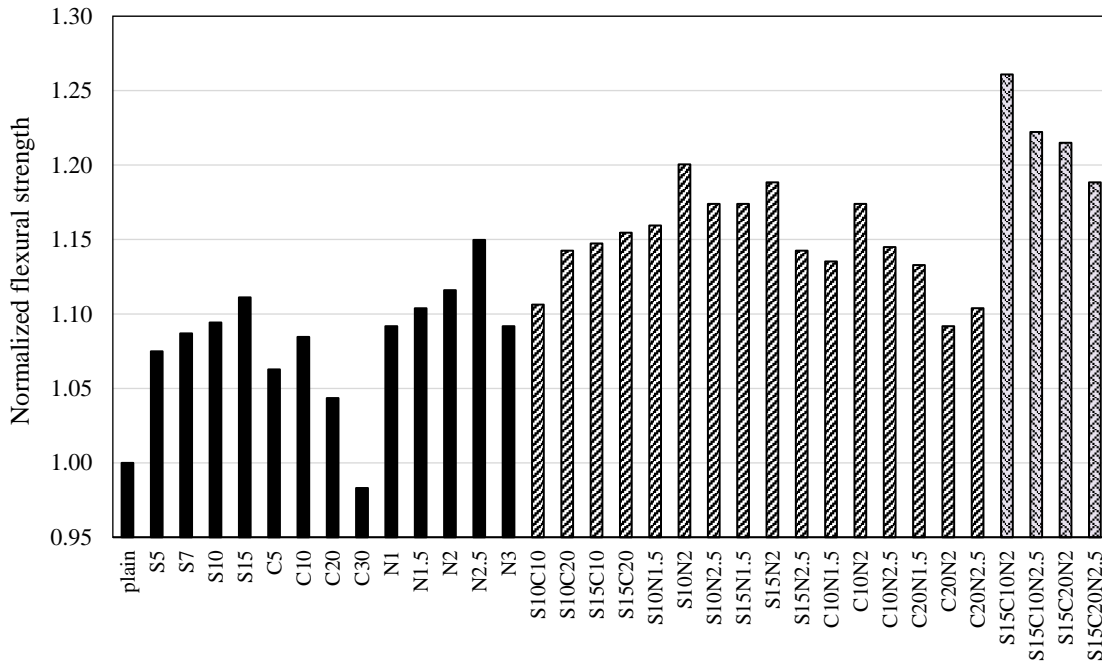


Fig. 4 Normalized flexural strength diagram according to the control sample

about 18.3% better than the control sample. Among the samples containing silica fume and copper slag, the combination of 15% silica fume and 20% copper slag had the best performance and increased the tensile strength by about 12%. Furthermore, the combination of different amounts of copper slag and nano-silica improved this strength by 7 to 16%, and the highest increase in tensile strength was related to the mixed design with a combination of 10% of copper slag and 1.5% of nano-silica. As can be seen in Fig. 3, the tensile strength is significantly improved in the mixtures containing three cement substitutes. The final optimal mix for the sample contains 15% silica fume, 10% copper slag, and 2% nano-silica, in which the tensile strength increased by about 23% compared to the control sample.

4.3 Flexural strength

In Tables 5 and 6, the results of the three-point bending test and in the diagram of Fig. 4, the normalized flexural strengths of the mix designs are shown according to the control sample. Among the four mixes containing different amounts of silica fume, the mix design with 15% silica fume by increasing about 11% in flexural strength had the best performance. Furthermore, among nine mixes containing different amounts of copper slag or nano-silica, the mixes with 10% copper slag and 2.5% nano-silica, by increasing about 9 and 15% in flexural strength, respectively, were able to have the best performance.

In samples with two cement substitutes, the mix design containing 10% silica fume and 2% nano-silica had the best flexural strength, which was about 20% higher than the control sample. Furthermore, in the mix include of 15% of silica fume and 20% of copper slag, the flexural

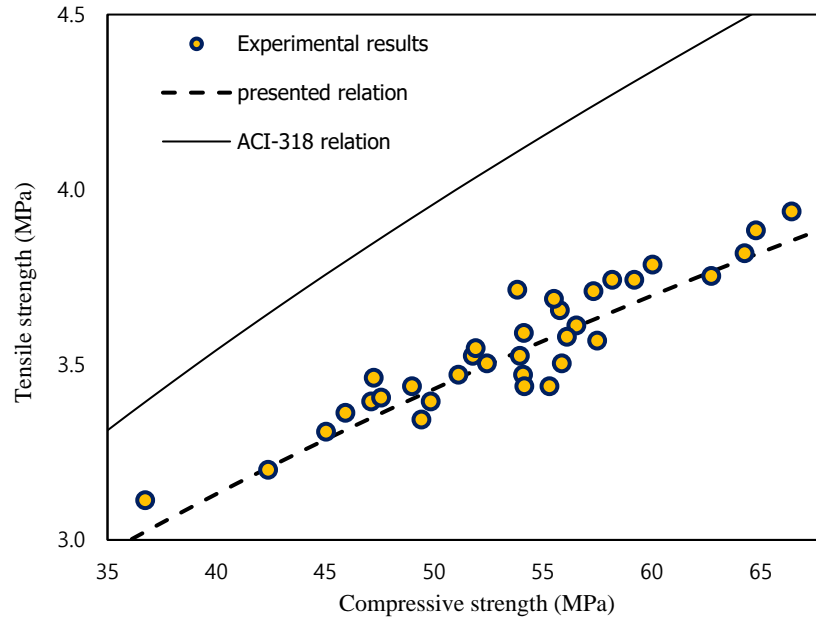


Fig. 5 Comparison of the relation presented in this study for tensile strength with the ACI318-14 relation (2015)

strength improved by about 15.5%, and in the case of a combination of 10% of copper slag and 2% of nano-silica, this strength improved by about 17.4%. In the mix designs with three cement substitutes, such as compressive and tensile strengths, the best mix included 15% silica fume, 10% copper slag, and 2% nano-silica. In this mix, the flexural strength increased by about 26% compared to the control sample.

4.4 Presenting a relation for predicting tensile and flexural strengths

In equal compressive strength, the tensile and flexural strengths of the cementitious composites are different from their corresponding values in the normal concrete. ACI318-14 Code (2015) provides the following relationship to determine the tensile strength from its compressive strength.

$$f_t = \lambda \times 0.56 \times \sqrt{F_c} \quad (2)$$

In the above relationship, F_c is the compressive strength of the cylindrical sample, and f_t is its tensile strength in MPa.

Fig. 5 compares the results of the proposed relation in this study, the predicted results of the ACI318-14 relationship (2015), and the results of this laboratory study. As shown in the figure, there is a far difference between the experimental results and the calculated results from the ACI318-14 relation (2015). Therefore, this relationship cannot predict the tensile strength of cementitious composites using the compressive strength obtained in the laboratory, and thus a special relation must be provided for it. In this research, by examining 34 different mix designs, using nonlinear analysis and regression of the relevant data, the following relations have been

proposed to determine the tensile and flexural strengths of cementitious composites from their compressive strength.

$$F_t = 0.69(F_c)^{0.41} \quad R^2 = 0.865 \quad (3)$$

$$F_m = 1.18(F_c)^{0.41} \quad R^2 = 0.866 \quad (4)$$

In the above relations, F_c , F_t , and F_m parameters are the compressive strength of the cubic sample, the tensile strength, and the flexural strength of the cementitious composites in MPa, respectively. According to Fig. 5, the relation presented in this study can accurately predict the tensile strength of cementitious composite using its compressive strength.

According to Eq. (4), the correlation coefficient calculated for predicting the flexural strength is equal to 0.866, which shows that the proposed relation for determining the flexural strength also has good accuracy. Therefore, between the values predicted from this relation and the experimental results, there is an acceptable coordination.

5. Conclusions

In this research, to decrease the amount of cement consumed in the production of cementitious composites, three cement replacement materials were used including copper slag, silica fume, and nano-silica in cases individually, a combination of two, and all three materials. According to the compressive, tensile, and flexural strength tests that were performed on the fiber-reinforced composite, the following results were obtained:

1- Based on the test results, among the mix designs with one cement substitute material, the best strength was related to the samples consisting of nano-silica. Among the different percentages of nano-silica replacement, the most optimal value was 2.5%. Among the different amounts of silica fume replacement, the best performance was related to the replacement percentage of 15%. Regarding the replacement percentage of copper slag, at the replacement percentage of 20%, the compressive strength reached its maximum value. On the other hand, in the replacement percentage of 10% of the cement weight with copper slag, the tensile and flexural strengths reached their maximum values.

2- In mixes with two cement substitute materials, the strengths increased significantly, and among all the mixes, the best strength was related to the combination of silica fume and nano-silica. The best strengths were obtained in the mix design with 10% silica fume and 2% nano-silica. In this design, the compressive, tensile, and bending strengths increased by 42, 18, and 20 percent, respectively, compared to the control sample.

3- It was observed that by combining the copper slag with silica fume and nano-silica in a cementitious composite, using cement content reduced, and its strengths also increased. In the mixes design containing three cement substitutes, the best sample was the mix with 15% silica fume, 10% copper slag, and 2% nano-silica. This mix improved the compressive, tensile, and flexural strengths by about 57, 23, and 26%, respectively.

4- Due to the different properties of ordinary concrete and cementitious composites, in this study, by examining 34 different mix designs and performing non-linear regression analysis, two relations have been presented that can predict the tensile and flexural strengths of cementitious composites only by determining the compressive strength of the mix.

Acknowledgments

This work was supported by Shahid Rajaei Teacher Training University under grant number 5973/70.

References

- Abna, A. and Mazloom, M. (2022), "Flexural properties of fiber reinforced concrete containing silica fume and nano-silica", *Mater. Lett.*, **316**, 132003. <https://doi.org/10.1016/j.matlet.2022.132003>.
- ACI 318-14 (2015), *Building code requirements for structural concrete and commentary on building code requirements for structural concrete*, American Concrete Institute.
- Afzali-Naniz, O. and Mazloom, M. (2019), "Assessment of the influence of micro-and nano-silica on the behavior of self-compacting lightweight concrete using full factorial design", *Asian J. Civil Eng.*, **20**(1), 57-70. <https://doi.org/10.1007/s42107-018-0088-2>.
- Amiri, M.M., Adabi, M., Darvishan, E. and Armanpour, A.H. (2022), "Investigation of effect of size and content of nano/SiO₂ on the strength and durability of RCC in freezing-thawing cycles", *Sharif J. Civil Eng.*, **38.2**(1.2), 145-154. <https://doi.org/10.24200/J30.2021.58139.2958>.
- ASTM-C494 (2001), *Standard specification for chemical admixtures for concrete*, American Society of Testing Materials
- ASTM-C496 (2002), *Standard test method for splitting tensile strength of cylindrical concrete specimens*, ASTM International, West Conshohocken, PA, USA.
- Aydin, A.C. (2007), "Self compactability of high volume hybrid fiber reinforced concrete", *Constr. Build. Mater.*, **21**(6), 1149-1154. <https://doi.org/10.1016/j.conbuildmat.2006.11.017>.
- BSI-12390 (2001), *BS EN 12390- Part 3: Testing hardened concrete: Compressive strength of test specimens*, BSI, London, UK.
- ASTM-C1609 (2019), *Standard test method for flexural performance of fiber-reinforced concrete (Using beam with third-point loading)*, ASTM International, West Conshohocken, PA, USA.
- Dos Anjos, M., Sales, A. and Andrade, N. (2017), "Blasted copper slag as fine aggregate in Portland cement concrete", *J. Environ. Management*, **196**, 607-613. <https://doi.org/10.1016/j.jenvman.2017.03.032>.
- Edwin, R.S., Gruyaert, E. and De Belie, N. (2022), "Valorization of secondary copper slag as aggregate and cement replacement in ultra-high performance concrete", *J. Build. Eng.*, **54**, 104567. <https://doi.org/10.1016/j.job.2022.104567>.
- Elahi, A., Basheer, P., Nanukuttan, S. and Khan, Q. (2010), "Mechanical and durability properties of high performance concretes containing supplementary cementitious materials", *Constr. Build. Mater.*, **24**(3), 292-299. <https://doi.org/10.1016/j.conbuildmat.2009.08.045>.
- Feng, Y., Yang, Q., Chen, Q., Kero, J., Andersson, A., Ahmed, H., Engström, F. and Samuelsson, C. (2019), "Characterization and evaluation of the pozzolanic activity of granulated copper slag modified with CaO", *J. Cleaner Product.*, **232**, 1112-1120. <https://doi.org/10.1016/j.jclepro.2019.06.062>.
- Gao, S., Tian, W., Wang, L., Chen, P., Wang, X. and Qiao, J. (2010), *Comparison of the mechanics and durability of hybrid fiber reinforced concrete and frost resistant concrete in bridge deck pavement*, ICCTP 2010: Integrated Transportation Systems: Green, Intelligent, Reliable. [https://doi.org/10.1061/41127\(382\)](https://doi.org/10.1061/41127(382)).
- Ghalehnovi, M., Rakhshanimehr, M. and Khodabakhshian, A. (2022), "The effect of waste marble powder and silica fume on the mechanical, environmental and economic performance of concrete", *Sharif J. Civil Eng.*, **37.2**(4.1), 33-47. <https://doi.org/10.24200/J30.2021.56505.2834>.
- Gideon, A.M. and Milan, R. (2021), "Effects of nitinol on the ductile performance of ultra high ductility fibre reinforced cementitious composite", *Case Studies in Constr. Mater.*, **15**, e00582. <https://doi.org/10.1016/j.cscm.2021.e00582>.
- Huang, K. (2001), "Use of copper slag in cement production", *Sichuan Cement*, **4**, 25-27.

- Jalal, M., Mansouri, E., Sharifipour, M. and Pouladkhan, A.R. (2012), "Mechanical, rheological, durability and microstructural properties of high performance self-compacting concrete containing SiO₂ micro and nanoparticles", *Mater. Design*, **34**, 389-400. <https://doi.org/10.1016/j.matdes.2011.08.037>.
- Kakooei, S., Akil, H.M., Jamshidi, M. and Rouhi, J. (2012), "The effects of polypropylene fibers on the properties of reinforced concrete structures", *Constr. Build. Mater.*, **27**(1), 73-77. <https://doi.org/10.1016/j.conbuildmat.2011.08.015>.
- Kashyap, V.S., Sancheti, G. and Yadav, J.S. (2023), "Durability and microstructural behavior of nano Silica-marble dust concrete", *Cleaner Mater.*, **7**, 100165. <https://doi.org/10.1016/j.clema.2022.100165>.
- Kong, D., Su, Y., Du, X., Yang, Y., Wei, S. and Shah, S.P. (2013), "Influence of nano-silica agglomeration on fresh properties of cement pastes", *Constr. Build. Mater.*, **43**, 557-562. <https://doi.org/10.1016/j.conbuildmat.2013.02.066>.
- Le Hoang, A. and Fehling, E. (2017), "Influence of steel fiber content and aspect ratio on the uniaxial tensile and compressive behavior of ultra high performance concrete", *Constr. Build. Mater.*, **153**, 790-806. <https://doi.org/10.1016/j.conbuildmat.2017.07.130>.
- Li, L., Huang, Z., Zhu, J., Kwan, A. and Chen, H. (2017), "Synergistic effects of micro-silica and nano-silica on strength and microstructure of mortar", *Constr. Build. Mater.*, **140**, 229-238. <https://doi.org/10.1016/j.conbuildmat.2017.02.115>.
- Lim, S., Lee, W., Choo, H. and Lee, C. (2017), "Utilization of high carbon fly ash and copper slag in electrically conductive controlled low strength material", *Constr. Build. Mater.*, **157**, 42-50. <https://doi.org/10.1016/j.conbuildmat.2017.09.071>.
- Mardani-Aghabaglou, A., Tuyan, M., Yilmaz, G., Ariöz, Ö. and Ramyar, K. (2013), "Effect of different types of superplasticizer on fresh, rheological and strength properties of self-consolidating concrete", *Constr. Build. Mater.*, **47**, 1020-1025. <https://doi.org/10.1016/j.conbuildmat.2013.05.105>.
- Massana, J., Reyes, E., Bernal, J., León, N. and Sánchez-Espinosa, E. (2018), "Influence of nano-and micro-silica additions on the durability of a high-performance self-compacting concrete", *Constr. Build. Mater.*, **165**, 93-103. <https://doi.org/10.1016/j.conbuildmat.2017.12.100>.
- Mazaheripour, H., Ghanbarpour, S., Mirmoradi, S. and Hosseinpour, I. (2011), "The effect of polypropylene fibers on the properties of fresh and hardened lightweight self-compacting concrete", *Constr. Build. Mater.*, **25**(1), 351-358. <https://doi.org/10.1016/j.conbuildmat.2010.06.018>.
- Mazloom, M., Allahabadi, A. and Karamloo, M. (2017), "Effect of silica fume and polyepoxide-based polymer on electrical resistivity, mechanical properties, and ultrasonic response of SCLC", *Adv. Concrete Constr.*, **5**(6), 587-611. <https://doi.org/10.12989/acc.2017.5.6.587>.
- Mazloom, M., Karimpanah, H. and Karamloo, M. (2020), "Fracture behavior of monotype and hybrid fiber reinforced self-compacting concrete at different temperatures", *Adv. Concrete Constr.*, **9**(4), 375-386. <https://doi.org/10.12989/acc.2020.9.4.375>.
- Mazloom, M. and Mirzamohammadi, S. (2021), "Fracture of fibre-reinforced cementitious composites after exposure to elevated temperatures", *Mag. Concrete Res.*, **73**(14), 701-713. <https://doi.org/10.1680/jmacr.19.00401>.
- Mazloom, M., Saffari, A. and Mehrvand, M. (2015), "Compressive, shear and torsional strength of beams made of self-compacting concrete", *Comput. Concrete*, **15**(6), 935-950. <https://doi.org/10.12989/cac.2015.15.6.935>.
- Mazloom, M. and Salehi, H. (2018), *The relationship between fracture toughness and compressive strength of self-compacting lightweight concrete*, IOP Publishing. <https://doi.org/10.1088/1757-899X/431/6/062007>.
- Mazloom, M., Salehi, H., Gholipour, M., Akbari-Jamkarani, M. and Afzali, F. (2022), *A Comprehensive Study of the Effects of Copper Slag on the Fresh and Hardened Properties of Different Cementitious Composites*, *Practice Periodical on Structural Design and Construction*, **27**(3), 05022003. [https://doi.org/10.1061/\(ASCE\)SC.1943-5576.000007](https://doi.org/10.1061/(ASCE)SC.1943-5576.000007).
- Mazloom, M., Soltani, A., Karamloo, M., Hassanloo, A. and Ranjbar, A. (2018), "Effects of silica fume, superplasticizer dosage and type of superplasticizer on the properties of normal and self-compacting concrete", *Adv. Mater. Res.*, **7**(1), 45-72. <https://doi.org/10.12989/amr.2018.7.1.045>.

- Murari, K., Siddique, R. and Jain, K. (2015), "Use of waste copper slag, a sustainable material", *J. Mater. Cycles Waste Management*, **17**(1), 13-26. <https://doi.org/10.1007/s10163-014-0254-x>.
- Nili, M. and Ehsani, A. (2015), "Investigating the effect of the cement paste and transition zone on strength development of concrete containing nanosilica and silica fume", *Mater. Design*, **75**, 174-183. <https://doi.org/10.1016/j.matdes.2015.03.024>.
- Saha, S., Rajasekaran, C. and Vinay, K. (2017). "Use of concrete wastes as the partial replacement of natural fine aggregates in the production of concrete", *Proceedings of the Global Civil Engineering Conference*. https://doi.org/10.1007/978-981-10-8016-6_32.
- Salehi, H. and Mazloom, M. (2018), "Experimental and numerical studies of crack propagation in self-compacting lightweight concrete", *Modares Mech. Eng.*, **18**(6), 144-155.
- Salehi, H. and Mazloom, M. (2019), "Effect of magnetic-field intensity on fracture behaviors of self-compacting lightweight concrete", *Mag. Concrete Res.*, **71**(13), 665-679. <https://doi.org/10.1680/jmacr.17.00418>.
- Salehi, H. and Mazloom, M. (2019), "Opposite effects of ground granulated blast-furnace slag and silica fume on the fracture behavior of self-compacting lightweight concrete", *Constr. Build. Mater.*, **222**, 622-632. <https://doi.org/10.1016/j.conbuildmat.2019.06.183>.
- Salehi, H. and Mazloom, M. (2021), "Studying the effect of silica fume on the fracture toughness and fracture energy of self-compacting lightweight concrete", *J. Civil Environ. Eng.*, **53**(1), 139-151. DOI: <https://doi.org/10.22034/JCEE.2021.43557.1985>.
- Scrivener, K.L. and Kirkpatrick, R.J. (2008), "Innovation in use and research on cementitious material", *Cement Concrete Res.*, **38**(2), 128-136. <https://doi.org/10.1016/j.cemconres.2007.09.025>.
- Shajil, N., Srinivasan, S. and Santhanam, M. (2013), "Self-centering of shape memory alloy fiber reinforced cement mortar members subjected to strong cyclic loading", *Mater. Struct.*, **46**(4), 651-661. <https://doi.org/10.1617/s11527-012-9923-1>.
- Tangtakabi, A., Ramesht, M.H., Golsoorat Pahlaviani, A. and Pourrostam, T. (2022), "Optimum use of micro silica in reducing corrosion reinforcing steel of marine concrete structures", *Amirkabir J. Civil Eng.*, **54**(8), 2953-2968. <https://doi.org/10.22060/CEEJ.2022.18954.7008>.
- Tiwary, A.K. and Bhatia, S. (2022), "A study incorporating the influence of copper slag and fly ash substitutions in concrete", *Mater. Today: Proceedings*, **48**, 1476-1483. <https://doi.org/10.1016/j.matpr.2021.09.293>.
- van Zijl, G.P., Wittmann, F.H., Oh, B.H., Kabele, P., Toledo Filho, R.D., Fairbairn, E.M., Slowik, V., Ogawa, A., Hoshiro, H. and Mechtcherine, V. (2012), "Durability of strain-hardening cement-based composites (SHCC)", *Materials and structures*. **45**(10), 1447-1463. <https://doi.org/10.1617/s11527-012-9845-y>.
- Wang, Z., Zhang, T. and Zhou, L. (2016), "Investigation on electromagnetic and microwave absorption properties of copper slag-filled cement mortar", *Cement Concrete Compos.*, **74**, 174-181. <https://doi.org/10.1016/j.cemconcomp.2016.10.003>.
- Yu, K.Q., Yu, J.T., Dai, J.G., Lu, Z.D. and Shah, S.P. (2018), "Development of ultra-high performance engineered cementitious composites using polyethylene (PE) fibers", *Constr. Build. Mater.*, **158**, 217-227. <https://doi.org/10.1016/j.conbuildmat.2017.10.040>.